

Synthesis and characterization of a low- T_g photorefractive composite

In Kyu Moon^{a,*}, Chil-Sung Choi^b, Nakjoong Kim^{b,**}

^a Information and Electronic Materials Lab., Environment and Energy Division, Korea Institute of Industrial Technology, Chungnam 330-825, Republic of Korea

^b Department of Chemistry, Hanyang University, Seoul 133-791, Republic of Korea

ARTICLE INFO

Article history:

Received 10 March 2008

Received in revised form

13 November 2008

Accepted 21 November 2008

Available online 28 November 2008

Keywords:

Photorefractive effect

Polysiloxanes

Triphenylamine

ABSTRACT

N,N'-Diphenyl-4-biphenylamine-substituted polysiloxane, PSX-bTPA was synthesized and characterized. We also studied the photoconductivity and the photorefractive properties of the polymeric photorefractive composite. The 50 μm thick photorefractive materials containing 30 wt% chromophore showed a diffraction efficiency 67% at 30 V/ μm , which corresponded to a speed of 2.6 s.

Published by Elsevier B.V.

1. Introduction

The recent interest in polymeric photorefractive (PR) composites is due to the flexible material design, high gain and diffraction efficiency that can be achieved with organic materials [1,2]. The PR effect is observed in materials that are both electro-optic (EO) and photoconducting. Nonuniform illumination of such a material results in the creation of photoexcited charges, which migrate out of the illuminated areas and eventually get trapped in the dark areas, giving rise to a spatially varying electric field (plus space-charge field). This space-charge field alters the index of refraction via the electro-optic effect [1].

The high performances observed for low glass transition temperature (T_g) doped polymers can be related to an efficient orientation of the EO chromophores in the space-charge field [2]. The most widely used photoconductive polymers were poly(*N*-vinylcarbazole) (PVK) [3–6]. However, PVK-based composites have suffered from the usage of the high applied voltages (~ 100 V/ μm) required for obtaining the high PR properties and the phase separation due to the high dopant concentration and a rigid framework of PVK, which are serious obstacles to the application.

Recently, Chun et al. [7,8] prepared a carbazole-substituted polysiloxane (PSX-Cz), with a lower T_g , which leads to a reduced concentration of required plasticizer in a photorefractive polymer composite and therefore a possible improvement of the pho-

totrefractive properties due to increased concentration of active groups. The advantages of this polymer include (i) good solubility in common organic solvents due to the presence of asymmetric alkyl groups at each Si center, (ii) low T_g due to flexible Si–O–Si linkages in the polymer main chain, and (iii) an excellent compatibility with polar molecules (e.g., EO chromophores) than that PVK composites [8]. However, a disadvantage of the PSX-Cz for use in PR composite was the slow response time of grating formation of the four-wave mixing (FWM) experimental due to probably the low photoconductivity. It increased the width of the site energy distribution and hence decreased the mobility by random of carbazole chromophores [9,10]. To solve these problems, the design criterion of the favorable hole-transporter is strongly needed with high charge carrier and good morphological stability. Among the hole-transporter, triphenylamine-like compounds than carbazole molecule have been proved to be excellent hole-transporting materials and have shown a wide range of practical applications. These class of materials offer many attractive properties such a high charge carrier and a softer than carbazole molecule due to the low ionization potentials (IP) energy [11] and the propeller-shaped phenyl groups on amine center. Therefore, IP level is an important parameter to consider when designing new, electron-donating polymers of PR material.

In our effort to synthesize new polymeric PR composite for application, we began with *N,N'*-diphenyl-4-biphenylamine as pendant group in the side chain of polysiloxanes (PSX-bTPA). Since the arylamine derivatives have a much low IP energy and large charge mobility [12,13] than the carbazole molecule, it would have a more important influence for the photoconducting polymer on the PR properties of the resulting polymeric PR

* Corresponding author. Tel.: +82 41 5898 522; fax: +82 41 5898 580.

** Corresponding author.

E-mail addresses: inkmoon@naver.com (I.K. Moon), kimnj@hanyang.ac.kr (N. Kim).

composite. PSX-bTPA is then believed that the preparation of these new PR polymeric composites could give not only highly photoconductivity but also the increased PR response time than that PSX-Cz composite. As mentioned above, the photoconductivity and the photorefractivity of this composite could be very useful for the development of polymeric PR materials. Complete synthetic details and device characterization are presented. The photoconductivity and PR properties of PSX-bTPA-containing composite are discussed in comparison with its PSX-Cz composite.

2. Experimental

2.1. Materials and characterization

Chemical reagents and solvents were obtained from Aldrich and poly(methylhydrosiloxane) ($M_w \sim 2000$) was purchased from United Chemical Technologies, and used after purification according to conventional methods. Toluene was distilled over sodium benzophenone under inert argon atmosphere. Methylene chloride and DMF were dried by distillation over CaH_2 . All reactions were carried out under inert nitrogen or argon atmosphere. 2-{3-[(E)-2-(Piperidino)-1-ethenyl]-5,5-dimethyl-2-cyclohexenylidene}malonitrile (P-IP-DC) synthesis and PSX-bTPA polymerization were carried out as cited in Ref. [7]. The chemical structure of the new materials was characterized by ^1H NMR spectrometry (Varian, INOVA, 400 MHz), FT-IR spectrometry (PerkinElmer, Paragon 500), and UV-vis spectrometry (Duksan Mechasys, Optizen III). The T_g of PSX-bTPA and PR composite was determined by differential scanning calorimetry (DSC, PerkinElmer DSC 7). The molecular weight and polydispersity were determined in THF solvent by a Waters GPC-410 calibrated with polystyrene standards.

2.2. Synthesis of biphenyl-4-yl-phenyl-amine (1)

Tris(dibenzylideneacetone)dipalladium(0) (Pd_2dba_3) (552 mg, 0.60 mmol), 1,1'-bis(diphenylphosphino)ferrocene (dppf) (505 mg, 0.91 mmol), and 4-bromobiphenyl (5 g, 21 mmol) were dissolved in 300 ml of dry toluene and stirred for 10 min. Sodium *tert*-butoxide (3.09 g, 32 mmol) and 3-methoxydiphenylamine (4.18 g, 21 mmol) were then added. The reaction mixture was warmed to 100°C for 12 h. The reaction mixture was partitioned between water and ether, and the aqueous layer was extracted with ether. The combined organic fractions were dried over MgSO_4 , and the solvent was evaporated under reduced pressure. Purification of the crude product by column chromatography (silica, with hexane/toluene (4/1) as an eluent) gave the product as pale yellow oil. The product yield was 83%. ^1H NMR (CDCl_3 , ppm) δ 3.74 (s, 3H), 6.55–7.56 (m, 18H). IR (KBr pellet, cm^{-1}): 2818 (methyl aromatic ether, $-\text{CH}_3$ str.).

2.3. Synthesis of 3-(biphenyl-4-yl-phenyl-amino)-phenol (2)

Boron tribromide (Eq. (1)) was added dropwise to a solution **1** (1.2 equiv.) in 300 ml of dry methylene chloride under stirring at -78°C , and the mixture was stirred at room temperature for 12 h. After completion of the reaction, the mixture was poured into crushed ice and extracted with methylene chloride two times. The combined organic fractions were dried over MgSO_4 , and the solvent was evaporated under reduced pressure. Purification was accomplished by column chromatography on silica gel with 10% ethyl acetate/hexane and passed 30% ethyl acetate/hexane to give 82% of title compound. ^1H NMR (CDCl_3 , ppm) δ 4.74 (br s, 1H), 6.55–7.56 (m, 18H). IR (KBr pellet, cm^{-1}): 3619 ($-\text{OH}$, str.).

2.4. Synthesis of (3-allyloxy-phenyl)-biphenyl-4-yl-phenyl-amine (3)

Compound **2** (3 g, 8.9 mmol), potassium carbonate (3.1 g, 22.3 mmol), and tricaprylmethylammonium chloride (one drop) was stirred at room temperature in 50 ml *N,N*-dimethylformamide (DMF) for 2 h. To this was added dropwise a solution of allyl bromide (1.1 g, 9.0 mmol) in DMF (5 ml) over 30 min. This stirred at 80°C for an additional 12 h. The result mixture was poured in water, extracted with 2×150 ml of methylene chloride. The organic layer was dried over MgSO_4 . After filtration and evaporation, the oil residue was chromatographed on silica gel with 5% ethyl acetate in hexanes to give 82% of the title compound. ^1H NMR (CDCl_3 , ppm) δ 4.41 (d, 2H), 5.24 (d, 1H), 5.36 (d, 1H), 5.90–6.04 (m, 1H), 6.54–7.59 (m, 18H).

2.5. Synthesis of PSX-bTPA

PSX-bTPA was prepared from the reaction of poly(methylhydrosiloxane) with **3** by the same procedure as previously described in poly[methyl-3-(9-carbazolyl)-propylsiloxane] (PSX-CZ) [7]. Yield: 63%. $T_g = 42^\circ\text{C}$. λ_{max} (nm, in CHCl_3): 324, M_n (M_w/M_n): 36,190 (1.62). ^1H NMR (CDCl_3 , ppm) δ -0.43 to 0.39 (br s, 3H), 0.40–1.69 (br m, 4H), 4.10–4.82 (br s, 2H), 6.00–8.02 (br m, 18H).

2.6. Device preparation

In this work, low- T_g photorefractive material was prepared by doping the optically anisotropic chromophore, P-IP-DC, into photoconducting polymer matrix, PSX-bTPA sensitized by C_{60} . The composition of polymeric composite was PSX-bTPA (as a hole-transporter):P-IP-DC (as a EO chromophore):butyl benzyl phthalate (BBP, as a plasticizer): C_{60} (as a photosensitizer) = 64:30:5:1 by wt% (composite's $T_g = 30^\circ\text{C}$). The device was prepared by sandwiching the softened composite between two ITO coated glass plates. The thickness of active layer was $50 \mu\text{m}$.

2.7. Optical measurement

All optical measurements were carried out at the composite's T_g by illumination at a wavelength of 633 nm. The photogeneration efficiency, ϕ , which is defined as conversion efficiency from absorbed photons to free carriers, was measured by the xerographic discharge method [14]. The photoinduced decay of surface potential was measured by a noncontact electrostatic voltmeter. The quantum efficiency of photogeneration ϕ can be calculated by the following equation:

$$\phi = - \left(\frac{\varepsilon \varepsilon_0}{d I_0} \right) \left(\frac{dV}{dt} \right)_{V_i} \quad (1)$$

where ε is the dielectric constant, d is the sample thickness, I_0 is the photon flux, and V_i the surface potential at the onset of illumination. Also, the photoconductivity measurements ($\lambda = 632.8 \text{ nm}$) were performed on about $100 \mu\text{m}$ thick samples sandwiched between ITO electrodes at a 13 mW/cm^2 using a photocurrent method [15].

The EO properties of the polymeric composites were determined using the transmission ellipsometric method [16,18]. The value of Δn of composite was determined from the variation of the transmitted intensity (T) through the crossed polarizers upon the application of the electric field. These data from the transmission ellipsometer experiments can be used to predict both the steady-state holographic contrast of the photorefractive composite, and to quantify the rotational freedom of the chromophores within the sample.

The diffraction efficiency of photorefractive material was determined by the degenerate four-wave mixing (DFWM) experiment [16]. Two coherent laser beams at the wavelength of 632.8 nm were irradiated on the sample in the tilted geometry with the incident angle of 30° and 60° with respect to sample normal. The writing beams both were *s*-polarized and had the equal intensity of 60 mW/cm². The recorded photorefractive grating was read out by a *p*-polarized counter-propagating beam. Attenuated reading beam with the very weak intensity of 0.1 mW/cm² was used. The internal diffraction efficiency (η_{int}) of photorefractive material was determined from the equation:

$$\eta_{\text{int}} = \frac{I_{\text{R,diffracted}}}{I_{\text{R,diffracted}} + I_{\text{R,transmitted}}} \quad (2)$$

where $I_{\text{R,diffracted}}$ and $I_{\text{R,transmitted}}$ are the diffracted and transmitted intensities of reading beam, respectively.

3. Results and discussion

3.1. Synthesis and characterization

As shown in Scheme 1, all monomers and polymer have been easily prepared from 3-methoxydiphenylamine. In the first approach we synthesized the arylamine derivatives. It is a derivative of one of the most common organic hole-conductors. The arylamine monomer is synthesized in three steps starting from 3-methoxydiphenylamine. First, the formation of arylamine is achieved by a palladium catalyzed C–N coupling reaction. **1** is obtained in high yield (83%) after purification by column chromatography. Demethylation of **1** with BBr₃/methylene chloride gave the **2**, which were further allylated with allyl bromide under a base condition to yield the allyl-substituted arylamine **3** (see Scheme 1).

The main merit of polysiloxanes is a very low T_g due to the larger bond angles and bond lengths associated with the siloxane backbone relative to those of vinyl polymers or polyethers. 3-Substituted polysiloxane, PSX-bTPA was prepared from the hydrosilylation reaction of **3** molecule with poly(methylhydrosiloxane) by the platinum catalyst. Hydrosilylation of **3** was carried out in freshly dried toluene at 100 °C for 2 days. As expected, the structure of the PSX-

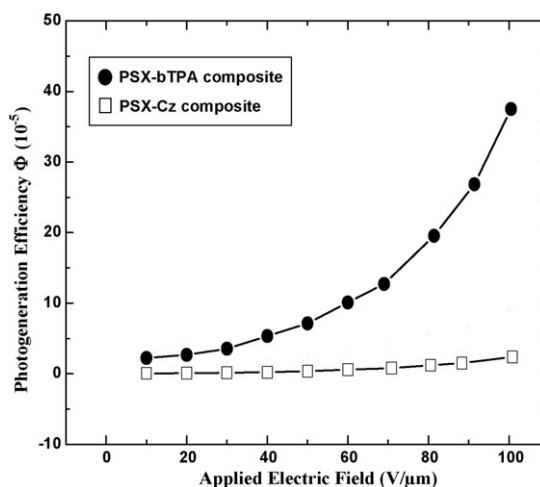
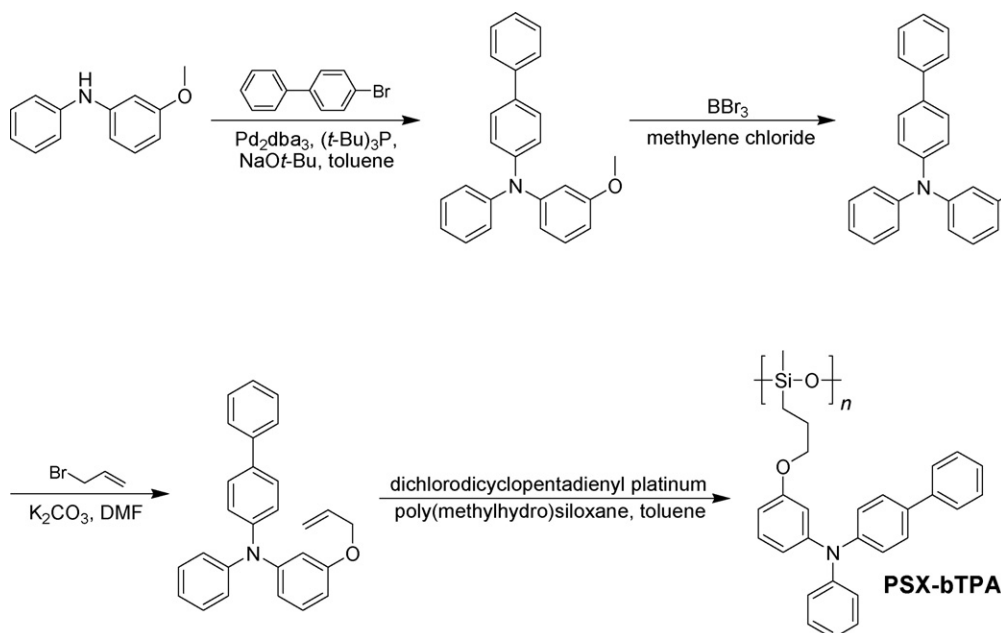


Fig. 1. Photogeneration efficiency of PSX-bTPA (●) and PSX-Cz (□) composites as a function of an electric field.

bTPA was confirmed by IR and H NMR spectroscopy. The starting Si–H peak at 2108 cm⁻¹ was completely disappeared by hydrosilylation when reaction times over 48 h. Also, the H NMR spectrum of PSX-bTPA exhibited broad resonance peaks typical polymers. The absorption peaks at allyl-groups form **3** in the H NMR spectrum of the polymer. The resulting copolymers are soluble in common organic solvents. The number-average molecular weights of PSX-bTPA, using THF as the eluent and polystyrene standards for calibration are 23,700 g/mol with a polydispersity index of around 1.62. The UV–vis absorption bands of polymer PSX-bTPA, centered at about 324 nm in CHCl₃, can be attributed to the **3** moiety.

3.2. Photoconductivity and electro-optic properties

In order to determine the variation of photogeneration by adding the P-IP-DC chromophore into PSX-bTPA, photogeneration efficiency of PSX-bTPA composite compared with PSX-Cz composite (PSX-Cz:P-IP-DC:BBP:C₆₀ = 64:30:5:1 by wt%). As shown in Fig. 1, the photogeneration efficiency of PSX-bTPA and PSX-Cz composite



Scheme 1. Synthetic routes of polymer.

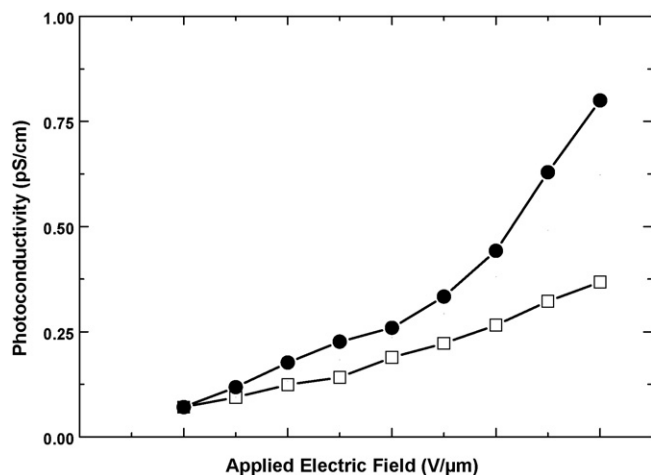


Fig. 2. Photoconductivity of PSX-bTPA (●) and PSX-Cz (□) composites as a function of an electric field.

was calculated to be 7.14×10^{-5} and 0.37×10^{-5} under field strength of $50 \text{ V}/\mu\text{m}$, respectively. Compared to the PSX-Cz composite, PSX-bTPA composite displays ~ 19 -fold higher quantum efficiency. The quantum efficiency showed the electric field dependence which can be simulated theoretically by Onsager's model of the geminate-pair dissociation.

The electric field dependence of the photoconductivity at $13 \text{ mW}/\text{cm}^2$ is shown in Fig. 2. Both samples exhibit almost linear induced-electric field dependence. As shown in Fig. 2, photoconductivity measurements on two samples yield photoconductivities σ_{ph} $0.79 \text{ pS}/\text{cm}$ for PSX-bTPA composite and $0.36 \text{ pS}/\text{cm}$ for PSX-Cz composite at an applied electric field of $50 \text{ V}/\mu\text{m}$. The σ_{ph} of PSX-bTPA composite is about two times higher than that of PSX-Cz composite. These results agreed to the initial expectation that the PSX-bTPA has larger photoconductivity than the corresponding PSX-Cz. This result may be explained by a previously reported study [4].

Probably, the depth of chromophore HOMO as a hole trap can affect the charge mobility, and then turn affects the photoconductivity, with lower photoconductivity for deeper hole traps. In our case, the energy level of the sensitizer LUMO is higher than that of the charge-transporter HOMO, i.e., the IP of PSX-bTPA is lower than that of PSX-Cz, so that the PSX-bTPA energy level acts as a trap for the EO chromophore holes and leads to the observed increase in mobility by several orders of magnitude of the PSX-Cz. Semi-empirical IP calculations were run on an Indigo-2 Silicon Graphics workstation by using the VAMP (V 6.5) software, supplied by Oxford Molecular-Accelrys. The structures of the molecules were fully optimized *in vacuo* by SCF calculation with AMI method according to literature [17]. The IP of (propyloxy-phenyl)-biphenyl-4-yl-phenylamine was about 7.78 eV , which was lower value than that 8.25 eV of *N*-propylcarbazole. If the HOMO of the EO chromophore is higher in energy than that for the charge-transport molecule, the EO chromophore can donate an electron from its HOMO to a nearby the charge-transport molecule HOMO. Thus, the EO chromophore acts as a trap for holes. That is the depth of the EO chromophore HOMO as a hole trap can affect the charge mobility, and then turn affects the photoconductivity, with lower photoconductivity for deeper hole traps. The HOMO level of PSX-bTPA is very close to that of P-IP-DC. Therefore, the lower HOMO level of PSX-bTPA, compared with PSX-Cz, may lead to larger photoconductivity, which is consistent with our experiment result. This fact suggests that PSX-bTPA can lead to a higher photoconductivity.

As shown in Fig. 3, the birefringence (Δn) of composites containing the P-IP-DC chromophore increased quadratically with

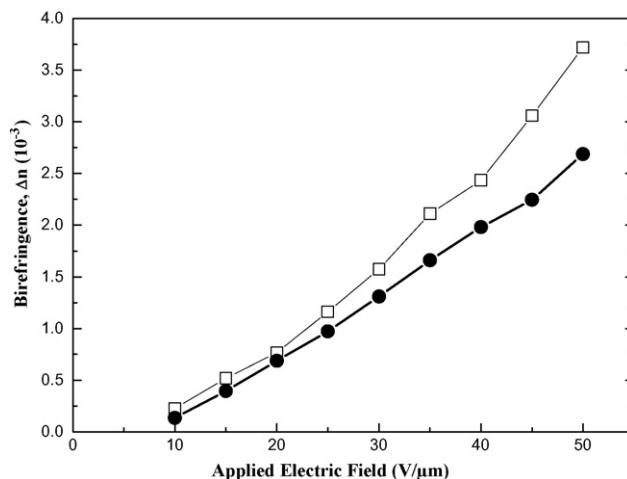


Fig. 3. Electric field-induced birefringence of PSX-bTPA (●) and PSX-Cz (□) composites versus applied electric fields.

increasing applied field. At an applied potential of $50 \text{ V}/\mu\text{m}$ ($I = 10 \text{ mW}/\text{cm}^2$), $\Delta n = 3.72 \times 10^{-3}$ for PSX-bTPA composite and $\Delta n = 2.69 \times 10^{-3}$ for PSX-Cz composite, which are sufficiently large values for the preparation of efficient photorefractive materials. The high EO properties may be due to a large dipole moment as well as high polarizability anisotropy of P-IP-DC chromophore associated with the effective conjugation along the polyene type [8]. Since the chromophores are rotating within an amorphous medium, they typically exhibit a nonexponential dynamic behavior.

3.3. Photorefractive properties

The T_g is of outstanding important for today's high-performance PR polymers. Orientational enhancement effect [1–3] is basically due to the possibility of in situ orienting the EO chromophores by means of the total electric field, which emerges in the systems through superposition of the externally applied field E_{ext} with the internal space-charge field E_{sc} , the latter being effected by the PR response of the material. As a result, the PR refractive index modulation Δn originates mostly from an orientational birefringence. In order to take real advantage of the promising photoconducting properties of PSX-bTPA, T_g and a photosensitizer for charge generation. The goal of this study was then to compare the steady-state PR performance of the PSX-bTPA composite with PSX-Cz composite with similar T_g and the same chromophores and content.

DFWM experiments were carried out during recording of PR grating in the materials investigated. The PR properties in PSX-bTPA and PSX-Cz, polymeric composites were prepared from a mixture of the photoconducting polymer (64 wt%), EO chromophore (30 wt%), BBP plasticizer (5 wt%), C_{60} (1 wt%). The T_g values of the PSX-bTPA and PSX-Cz composites from the DSC data were $T_g = 30$ and 28°C , respectively, which assure the facile orientation of the EO chromophore at temperatures around T_g . The PR properties of the current polymer composites were evaluated by the diffraction efficiency (η). The diffraction efficiency (η) of composite shows an oscillatory behavior, reflecting the sin square dependency [2,6]:

$$\eta = \sin^2[C\Delta n] \quad (3)$$

where Δn is the refractive index modulation and C is the constant determined by a wavelength, thickness, geometry of sample and so on. The values of the maximum diffraction (η_{max}) of guest–host systems PSX-bTPA and PSX-Cz were 67% and 85% at $30 \text{ V}/\mu\text{m}$, respectively. These composite showed high diffraction efficiencies under low external electric field (Fig. 4). As was pointed out in Section 1, PR characteristics are complex phenomena which are

Table 1
Thermal and optical properties of polymeric photorefractive composites.

Composite	Composite's T_g ($^{\circ}\text{C}$)	Φ ($\times 10^{-5}$)	σ (pS/cm)	η (%)	$\eta(t)$ (s)
		[@ 50 V/ μm]		[@ 30 V/ μm]	
PSX-bTPA composite	30	7.14	0.79	67	2.2
PSX-Cz composite	28	0.37	0.36	85	5.5

influenced by the properties of each component and interactions between the components. This is due to the applied voltage influencing both the (re)orientation of the EO chromophore and the E_{Sc} within the composite.

One of the major properties of PR composites has been the response time of the diffraction efficiency. This parameter is very important for real application such as real-imaging processing. To investigate the fast response time of PR devices, we measured the induced-electric field of the response time of the diffraction efficiency. After 200 s, the other writing beam was applied and the diffracted reading beam was monitored. Time constants τ_1 were calculated by fitting the evolution of the growth of the diffraction signal, $\eta(t)$ [4]. PSX-bTPA has a faster response time of 2.6 s, whereas PSX-Cz has a slower response time of 5.5 s at the same applied field ($E = 30 \text{ V}/\mu\text{m}$) (Fig. 5). These faster responses are also ascribed to faster drift mobility of hole in PSX-bTPA composite

due to lower IP of the triphenylamine moiety in PSX-bTPA [18,19]. This difference is believed to arise from the difference in both the reorientation speed and the photoconductivity. The HOMO of the chromophore acts as a trap for holes due to the higher in energy than that for the HOMO of the charge-transport molecule [18]. In other word, explanation involves the more electron-donating character of the triphenylamine group relative to the carbazole group, thereby turn affects the photoconductivity, with lower photoconductivity for deeper hole traps. The results of these composites are listed in Table 1.

Among the many polymeric PR materials reported so far, guest–host systems based on a photoconducting polymers doped with EO chromophores have been extensively studied due to their promising properties. However, guest–host systems often suffer from the phase separation associated with the limited compatibility of polar chromophore with the photoconducting polymer and the high concentration of dopants [14]. Our polymer sample containing 30 wt% of P-IP-DC chromophore shows the good phase stability. The optical clarity of device has been retained over several months when stored at room temperature, which was confirmed by an UV–vis spectrometer. This may arise partially from the good compatibility of P-IP-DC chromophore with matrix polymer, which can be assured from the observation that the melting peak of P-IP-DC chromophore disappears completely in PR polymer composite by DSC. Furthermore, the lower concentration of dopants in our material may also contribute to the device stability, being compared with typical PR guest–host system [3–6]. Plasticizer was added a small quantity in our composites, due to the relatively low T_g (51°C) of PSX-bTPA and PSX-Cz. T_g of our PR polymer can be lowered to room temperature simply by adding the chromophore, differently from PVK composite which generally contain plasticizer in the range of 10–20 wt%.

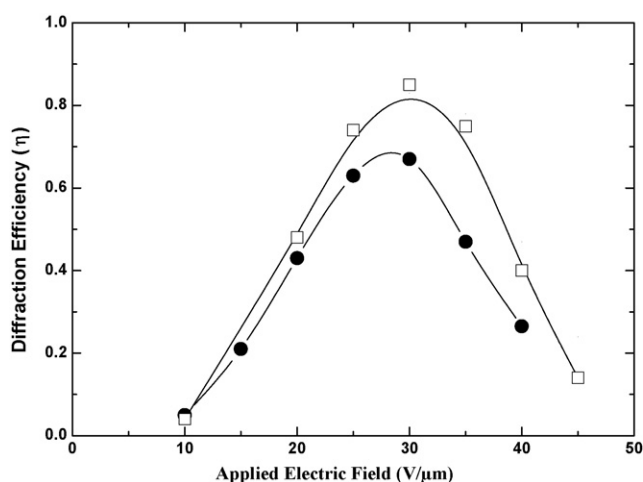


Fig. 4. Diffraction efficiency of PSX-bTPA (●) and PSX-Cz (□) composites as a function of an electric field.

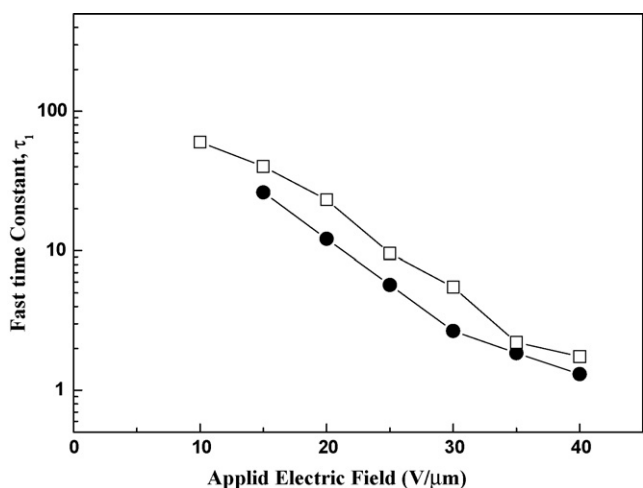


Fig. 5. The response time of the diffraction efficiencies of PSX-bTPA (●) and PSX-Cz (□) composites as a function of an electric field.

4. Conclusion

Here we presented PSX-bTPA for PR materials with a long-term stability. Comparing the photogeneration and photoconductivity of PSX-Cz composite with that of the PSX-bTPA composite shows that the former is about 19-fold and two times larger, respectively. The PSX-bTPA composite showed a high diffraction efficiency of 67% in moderate electric field of 30 V/mm, with a response time of the diffraction efficiency of 2.6 s at T_g .

Acknowledgments

The present work was supported by the Korea Science and Engineering Foundation (KOSEF) of the Korea government (MEST) (No. R11-2007-050-01003-0) and Research fund of Hanyang University (HYU-2008-T).

References

- [1] F. Würthne, R. Wortmann, K. Meerholz, Chem. Phys. Chem. 3 (2002) 17–31.
- [2] O. Ostroverkhova, W.E. Moerner, Chem. Rev. 104 (2004) 3267–3314.
- [3] K. Meerholtz, B.L. Volodin, B. Sandalphon, N. Kippelen, Peyghambarian, Nature 371 (1994) 497–500.
- [4] M. Wright, M.A. Díaz-García, J.D. Casperson, M. DeClue, W.E. Moerner, Appl. Phys. Lett. 73 (1998) 1490–1492.

- [5] F. Wurthner, S. Yao, J. Schilling, R. Wortmann, M. Redi-Abshiro, E. Mecher, F. Gallego-Gomez, K. Meerholz, *J. Am. Chem. Soc.* 123 (2001) 2810–2814.
- [6] S.J. Zilker, *Chem. Phys. Chem.* 1 (2000) 72–87.
- [7] H. Chun, I.K. Moon, D.-H. Shin, N. Kim, *Chem. Mater.* 13 (2001) 2813–2817.
- [8] H. Chun, I.K. Moon, D.-H. Shin, S. Song, N. Kim, *J. Mater. Chem.* 12 (2002) 858–862.
- [9] R. Oshima, T. Uryu, M. Senō, *Macromolecules* 18 (1985) 1043–1045.
- [10] T. Uryu, H. Ohkawa, R. Oshima, *Macromolecules* 20 (1987) 712–716.
- [11] D.M. Pai, J.E. Yanus, M. Stolka, *J. Phys. Chem.* 88 (1984) 4707–4714.
- [12] C.W. Tang, S.A. Tang, V. Slyke, *Appl. Phys. Lett.* 51 (1987) 913–915.
- [13] P.M. Boresenberger, L. Pautmeier, H. Bässler, *J. Chem. Phys.* 94 (1991) 5447–5454.
- [14] J.S. Schildkraut, *Appl. Phys. Lett.* 58 (1991) 340–342.
- [15] Y. Zhang, T. Wada, L. Wang, H. Sasabe, *Chem. Mater.* 9 (1997) 2798–2804.
- [16] G. Bauml, S. Schoter, U. Hofmann, D. Harrer, *Opt. Commun.* 154 (1998) 75–78.
- [17] J.J.P. Stewart, *J. Comput. Chem.* 10 (1989) 221–264.
- [18] I.K. Moon, C.-S. Choi, N. Kim, *Polymer* 48 (2007) 3461–3467.
- [19] I.K. Moon, J.-W. Oh, N. Kim, *J. Photochem. Photobiol. A: Chem.* 194 (2008) 327–332.